Nanoscale

Gating effect by thousands of bubble-propelled micromotors in macroscale channels

Journal:	*Nanoscale*
Manuscript ID:	NR-ART-04-2015-002562.R1
Article Type:	Paper
Date Submitted by the Author:	28-May-2015
Complete List of Authors:	Teo, Wei Zhe; Nanyang Technological University, Chemistry and Biological Chemistry Wang, Hong; Nanyang Technological University, Division of Chemistry and Biological Chemistry Pumera, Martin; Nanyang Technological University, Chemistry and Biological Chemistry

Journal Name

ARTICLE

Gating effect by thousands of bubble-propelled micromotors in macroscale channels

Received 00th January 20xx,
Accepted 00th January 20xx

DOI: 10.1039/x0xx00000x

www.rsc.org/

Wei Zhe Teo,[a] Hong Wang [a] and Martin Pumera*[a]

Increasing interests in the utilization of self-propelled micro-/nanomotors for environmental remediation require the examination of their efficiency in the macroscale level. As such, we investigated the effect of micro-/nanomotors propulsion and bubbling on the rate of sodium hydroxide dissolution and the subsequent dispersion of OH^- ions across more than 30 cm, so as to understand how these factors might affect the dispersion of remediation agents in real systems which might require these agents to travel long distances to reach the pollutants. Experimental results showed that the presence of large numbers of active bubble-propelled tubular bimetallic Cu/Pt micromotors (4.5×10^4) induced a gating effect on the dissolution and dispersion process, slowing down the change in pH of the solution considerably. The retardation was found to be dependent on the number of active micromotors present in the range of 1.5×10^4 to 4.5×10^4 micromotors. At lower numbers (0.75×10^4), however, propelling micromotors did speed up the dissolution and dispersion process. The understanding of the combined effects of large number of micro-/nanomotors' motion and bubbling on its macroscale mixing behavior is of significant importance for future applications of these devices.

Introduction

The past decade saw huge interests and efforts placed on the development of self-propelled micro- and nanomotors as these synthetic devices showed promising applications in environmental remediation[1,2], natural resource discovery[3], drug delivery[4,5], and isolation of biological targets[6]. Motion of these micro- and nanomotors are powered mainly by self-electrophoresis, self-diffusiophoresis and bubble propulsion mechanisms.[7-9] Out of the three mechanisms, micro- and nanomotors that are propelled by the generation of bubbles attracted the most attention and examination as they exhibit the highest velocity and strongest power.[10-14] The catalytic reaction between the motors' surface and the supplied fuel give rise to the bubble formation and subsequent propulsion of the motor. At present, the most commonly utilized fuel in the works carried out thus far is hydrogen peroxide (H_2O_2), which decomposes into water (H_2O) and oxygen (O_2) quickly in the presence of platinum catalyst surface of the motors.[15-19]

Over the past few years, studies have demonstrated that rapid and efficient degradation of pollutants can be achieved with the introduction of micro-/nanomotors into the polluted water.[20-23] For example, Soler et al synthesized tubular bimetallic bubble-propelled micromotors, which consisted of metallic iron as the outer layer and platinum as the inner layer, for degradation of organic pollutants such as rhodamine 6G through the Fenton oxidation process.[22] They noted that the rate of removal of rhodamine 6G is approximately 12 times faster in the presence of the self-propelled micromotors than with stationary iron rolled-up tubes, and they attributed this observation to the enhanced mixing of the polluted solution caused by the moving micromotors. In another work, Orozco et al. discovered that, by placing PEDOT/Pt (PEDOT = poly(3,4-ethylenedioxythiphene)) microtubular motors into solutions containing organophosphate contaminants and decontaminating reagent hydrogen peroxide, the oxidative detoxification process was accelerated and they deduced that the enhanced degradation process observed was the consequence of mechanical mixing resulting from the motors' continuous movement and bubbling.[23] In a fundamental study conducted later, the same group provided strong evidence that the generation of bubbles from the micromotors indeed played a significant role in contributing to the mixing process.[24] Above the micro level, in the millimeter range, motors that are powered based on the Marangoni effect also exhibited their capability to facilitate the decontamination of polluted waters in macroscale (real-world size) level. Specifically, Zhao et al. reported the successful utilization of polysulfone (PSf) capsules loaded with sodium dodecyl sulfate (SDS) to hasten the aggregation of flocculated Fe^{3+} in a "maze" with channels that stretched over tens of centimeters.[25]

As we advance towards the real-world application of self-propelled micro-/nanomotors for environmental remediation, it seem necessary to determine how the mechanical agitation instigated by micro-/nanomotors propulsion and bubbling will affect mixing in the macroscale level. Therefore, herein we investigated the effect of adding varying amounts of active bubble-propelled micromotors on the rate of sodium

[a] Division of Chemistry & Biological Chemistry, School of Physical and Mathematical Sciences, Nanyang Technological University, 21 Nanyang Link, Singapore 637371, Singapore. E-mail: pumera.research@gmail.com

hydroxide (NaOH) dissolution and dispersion across long distances (> 30 cm). This was carried out by placing NaOH pellets at one end of a solution-filled channel and recording the time taken for pH to change at the opposite end. The solutions contained known numbers of propelling tubular bimetallic Cu/Pt micromotors, hydrogen peroxide, SDS and a pH indicator to observe the change in pH. We sought to infer, from this study, how bubbles formation and micromotors' motion could have an impact on the duration required for a remediation agent to reach target pollutants located tens of centimeters away in order to develop suitable protocols for micro-/nanomotors assisted clean-up of pollutants in real systems.

Experimental

Materials

Cyclopore polycarbonate membranes with conical-shaped pores of 2 µm in diameter were purchased from Whatman, USA (Cat. no. 7060-2511), colloidal graphite (isopropanol base) from Ted Pella, Inc. (Lot no. 12009-2, USA), hydrogen peroxide (H_2O_2; 35%) from Alfa Aesar, Singapore, methylene chloride and ethanol from Tedia, USA, platinum electrode (1 mm diameter) and Ag/AgCl/1M KCl electrode from CH instruments, USA, copper (II) sulfate ($CuSO_4 \bullet 5H_2O$, 98+%), sodium hydroxide (NaOH, Product No.: S8045) and sodium dodecyl sulfate (SDS, Product No.: L3771) from Sigma–Aldrich, platinum-plating solution from Technic Inc., USA, and bromothymol blue (BTB, Product No.: A17746) from Alfa Aesar. The chemicals were used as received and ultrapure water (18.2 MΩ cm) from a Millipore Milli-Q purification system was used throughout the experiments.

Apparatus

Electrochemical deposition was carried out using an Autolab PGSTAT 101 electrochemical analyser (Eco Chemie, Utrecht, The Netherlands) connected to a computer and controlled by NOVA version 1.8 software (Eco Chemie). A three-electrode configuration was adopted for the deposition procedure, in a customised electrochemical deposition cell at room temperature (23 °C). The auxiliary electrode was a platinum electrode while the reference electrode was an Ag/AgCl electrode. Ultrasonication process was carried out with a Fisherbrand FB 11203 ultrasonicator, and centrifugation was carried out with a Beckman Coulter Allegra 64R centrifuge. A Casio HD video-recorder was utilized for video recordings which were subsequently analysed using Nikon NIS-Elements software. Optical microscope Nikon Eclipse TE 50i was utilized to observe and count the number of propelling micromotors. Scanning electron microscopy (SEM) images were obtained using JEOL-7600F semi-in-lens FE-SEM in SEI mode with an accelerating voltage of 30.0 kV, at a working distance of 7.2 mm.

Preparation of Cu/Pt concentric bimetallic microtubes

Synthesis of the Cu/Pt concentric bimetallic microtubes was conducted using a modified electrochemical deposition procedure on a cyclopore polycarbonate template.[26] Prior to the electrochemical deposition experiment, colloidal graphite ink was applied on one side of the polycarbonate template using commercial cotton swabs and immediately attached to a piece of flattened aluminium foil. The template was then assembled into a customised electrochemical deposition cell and acted as the working electrode. After rinsing the template thoroughly with ultrapure water (18.2 MΩ cm), 1M $CuSO_4$ electrolyte was added to the cell to deposit an outer layer of Cu, along the pores of the template, galvanostatically at -4 mA for 450 s. Subsequently, the $CuSO_4$ electrolyte was removed, the cell rinsed thoroughly with ultrapure water and replaced with commercial platinum-plating solution. Following that, electrodeposition of the platinum segment was carried out at -4 mA for 450s. Upon completion of the deposition of microtubes, the electrochemical cell was disassembled and the template was washed with ultrapure water. The template was then ultrasonicated to remove the graphite layer before it was dissolved in methylene chloride. Ultrasonication was performed to aid the dissolution of the template and the electrochemically deposited microtubes were collected by centrifuging the solution at 6000 rpm for 3 min. The process of ultrasonication and centrifugation was repeated 3 times with methylene chloride to ensure complete dissolution of the template. Finally, impurities in the microtubes solution were removed by washing with ethanol and water for 2 times each, with 3 min of centrifugation at 6000 rpm following each washing step. The microtubes were stored in water at room temperature.

Operation of micromotors

Fresh 25 mL mixtures containing 4% H_2O_2, 1% SDS, 500 µL BTB solution and varying numbers of micromotors dispersed in ultrapure water were prepared for the study of micromotor gating effect on sodium hydroxide dissolution and dispersion in water. The BTB solution was made by dissolving 0.1 g of BTB powder in 100mL of 50% (v/v) ethanol and served as a pH indicator. The total number of propelling micromotors present in the 25 mL mixture was calculated first by placing 20 µL of the mixtures on a glass slide and counting them under an optical microscope ($n \geq 5$), before multiplying the average count by a factor of 1250. A Teflon maze made up of running pathways (width and depth = 1 cm) on a Teflon plate with dimensions of 42 cm by 26 cm by 2 cm was used for the experiments and a designated system of channels was constructed by blocking certain pathways of the maze using Teflon cubes (1 cm^3). The mixture was added to the system of channels before the start of each experiment and a sodium hydroxide pellet was subsequently placed at one end of the channel. The colour of the mixture changed as sodium hydroxide dissolved and spread towards the other end of the channel due to the presence of pH indicator (BTB) in the experiment. Videos of the dissolution and dispersion process were recorded by placing a video-recorder over the system of

channels to determine the time taken for the process to reach completion.

Results and discussion

We have studied the consequence of having large numbers (tens of thousands) of active bubble-propelled micromotors on the dissolution and dispersion rate of NaOH solid. The SEM image in Figure 1 displays a typical Cu/Pt concentric bimetallic micromotor used in this study. It can be observed from the image that the micromotors are conical in shape, measuring approximately 1 µm and 1.5 µm in diameters at the extreme ends, and about 8 µm in length.

A system of channels, in which the NaOH solid dissolution and dispersion measurements were carried out, consisted of a straight channel (length = 21 cm) connected to a circular channel (diameter = 15 cm) at one end created on a Teflon plate. The channels are 1 cm in both width and depth and they were filled with 25 mL of fresh pre-mixed solution, comprising of 4% H_2O_2, 1% SDS, 500 µL BTB solution (pH indicator) and known numbers of tubular bimetallic Cu/Pt micromotors, prior to the start of each experiment. Figure 2A shows the set-up of the system of channels before the addition of a NaOH pellet (average mass = 90.1 mg) at the bottom end of the system.

Upon introducing the solid NaOH pellet into the system, a colour change from yellow to blue in the pH indicator, which corresponded to an increase in pH of the solution was first observed in the solution nearer to the pellet and spread towards the opposite end as the OH^- ions released from the dissolution of NaOH were dispersed by convection and diffusion due to the build-up of an OH^- concentration gradient and density flux during the dissolution process. The rate of colour change decreased as time progressed, signifying a retardation in the OH^- dispersion process as the NaOH pellet became completely dissolved. Based on the experimental results, an average time of approximately 10 minutes was needed for the whole solution to turn from yellow to blue (sufficient OH^- ions to reach the top of the system) in the absence of bubble-propelled micromotors. The final alkaline solution obtained is illustrated in Figure 2B.

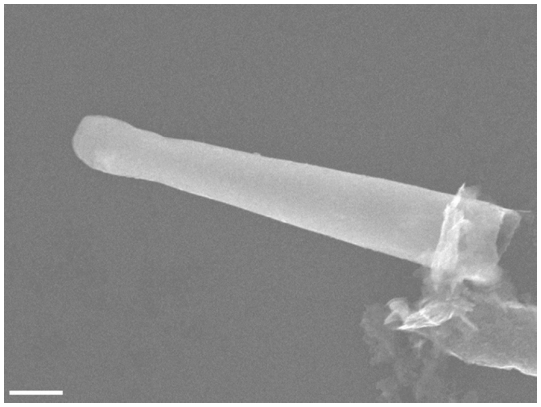

Figure 1. SEM image of the Cu/Pt micromotor. Debris found on the bottom right of the image belonged to the graphite ink which was applied to the polycarbonate template before the electrochemical deposition process. Scale bar represents 1 µm.

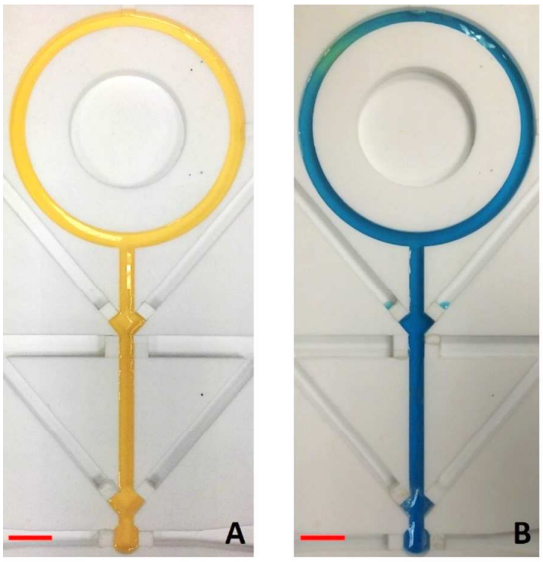

Figure 2. Photographs of the set-up of the system of channels with pre-mixed solution, comprising of 4% H_2O_2, 1% SDS and 500 µL BTB, (A) before the addition of a NaOH pellet and (B) when the solution became alkaline upon NaOH dissolution and dispersion after 10 minutes. Scale bars represent 3 cm for both (A) and (B).

With the incorporation of bubble-propelled micromotors into the pre-mixed solution, it was expected that the NaOH dissolution and dispersion process will be accomplished in a shorter time frame as demonstrated in previous studies.[20-23] However, on the contrary, we noticed a drastic reduction in the rate of colour change of the solution which contained around 4.5 x 10^4 active micromotors after 2 minutes from the addition of the NaOH pellet. The bubble-propelled micromotors seemed to have a gating effect on the OH^- ions, impeding their dispersion along the channels, down the concentration gradient. As depicted in Figure 3, the solution at top end of the system of channels (29.1 ± 6.5 %, n = 3) remained yellow even after 1 hour.

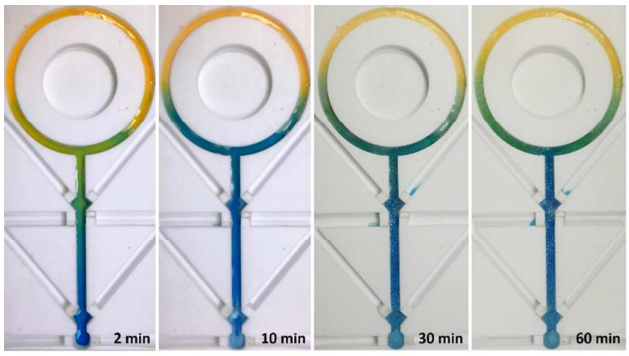

Figure 3. Gating effect of the propelling micromotors in macroscale channels. Images illustrating the change in pH of the pre-mixed solution containing 4% H_2O_2, 1% SDS, 500 µL BTB and 4.5 x 10^4 active micromotors as OH^- ions dispersed from the bottom of the system following NaOH (s) dissolution. The images were taken at 2, 10, 30 and 60 minutes from the addition of a NaOH pellet at the bottom of the system. An increase in pH was indicated by the change in the colour of the solution from yellow to blue. Width of channels = 1 cm.

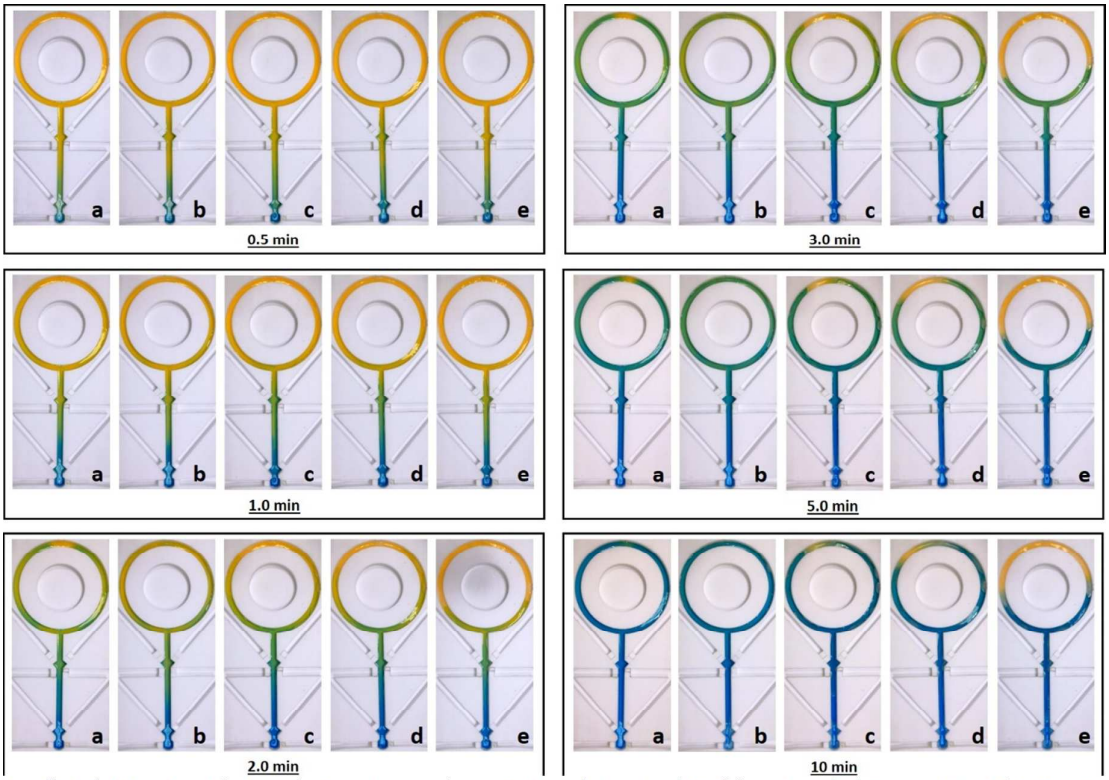

Figure 4. Gating effect of micromotors as function of active micromotors' concentration and time. *Snapshots of the pre-mixed solutions comprising of* 4% H_2O_2, 1% SDS, 500 µL BTB and various numbers of micromotors, taken at various times of the experiment, starting from 0.5 min after the addition of a NaOH pellet at the bottom of the system. The pre-mixed solutions contained (a) zero, (b) 0.75 x 10^4, (c) 1.50 x 10^4, (d) 2.25 x 10^4 and (e) 4.50 x 10^4 propelling micromotors respectively. Changes in the colour of the solution corresponded to an increase in pH of the solution. Width of channels = 1 cm.

We investigated this phenomenon further by altering the amount of active micromotors present in the pre-mixed solution and images of the system at various times of the experiment are displayed in Figure 4. The amount of propelling micromotors present in the fresh pre-mixed solution in samples **a** to **e** illustrated in the figure is 0 (**a**), 0.75 x 10^4 (**b**), 1.50 x 10^4 (**c**), 2.25 x 10^4 (**d**), and 4.50 x 10^4 (**e**) respectively. From the data collected, it can be seen that in the first minute of the experiment, the rate of NaOH dissolution and dispersion were similar in all the samples. However, subsequent snapshots taken after 2 minutes revealed that the area of yellow solution remaining (did not experience an increase in pH) in the channels started to differ between the samples, especially between the control (sample **a**) and samples **c** to **e.** It was found that the percentage of yellow solution remaining 5 minutes after placing the NaOH pellet increased from 3.8 % (**a**) to 7.9 % (**c**), 14.7 % (**d**) and 40.8 % (**e**) respectively. These observations suggest that micromotors were responsible for the gating effect on the dispersion of OH^- ions and the intensity of the impedance was dependent on the amount of active micromotors available in the solution. In addition, the concentration gradient and density flux present during the first minute of the experiment might be too strong, resulting in insignificant retardation of OH^- dispersion by the active micromotors. On the other hand, the NaOH dissolution and dispersion process underwent a slight acceleration in the solution which contained 0.75 x 10^4 of propelling micromotors, with 100% change in solution colour observed after 5 minutes, suggesting that an optimal amount of active micromotors will result in favourable mixing of a solution in the macroscale level.

Comprehensive examination of the photographs acquired revealed that very small bubbles started to form a layer on top of the solution as the experiments proceeded and they often covered the entire width of the channel at the top of the system after a few minutes (Figure 5). In addition, the bubbles tend to accumulate above the area with little or no NaOH present (yellow solution) and their quantity decreased with the number of active bubble-propelled micromotors available in the solution as expected. This observation led us to believe that higher amounts of bubbling per unit area of solution and the subsequent formation of a more extensive layer of bubbles in solutions containing larger numbers of propelling

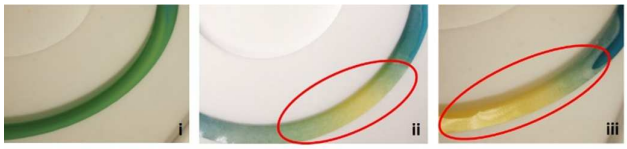

Figure 5. Close-up pictures showing portion of the system containing pre-mixed solutions with (i) 0.75 x 10^4, (ii) 2.25 x 10^4 and (iii) 4.50 x 10^4 propelling micromotors. Formation of a layer of bubbles on top of the solution are circled in red. The photographs were taken following the addition of NaOH pellet at the bottom of the system, at 5 minute mark for (i) and at 10 minute mark for (ii) and (iii). Width of channels = 1 cm.

micromotors attributed to the successful retardation of OH^- ions dispersion. However, at this juncture, we were unable to determine the mechanism behind the proposed gating effect in this work and we hope that this could be examined thoroughly in future works involving macroscale environmental remediation with micro-/nanomotors.

Conclusions

In this work, the presence of active bubble-propelled bimetallic Cu/Pt micromotors in large numbers (tens of thousands) were found to slow down the dissolution and dispersion of NaOH pellet in the macroscale level and this gating effect depended on the quantity of propelling micromotors available in the solution. The ejection of bubbles by propelling micromotors and the resulting bubble layer generated are probably the major contributors to the retardation of OH^- ions dispersion and they might affect the dispersion of remediation agents as well. More in-depth studies should be performed in the future to elucidate the exact mechanism which caused the gating effect so that we could improvise on the real-world applications of self-propelled micro-/nanomotors for environmental remediation.

Acknowledgements

M. P. acknowledge Nanyang Technological University and Singapore Ministry of Education Academic Research Fund AcRF Tier 1 (2013-T1-002-064, RG99/13) for the funding support.

References

1 J. Orozco, D. Vilela, G. Valdés-Ramírez, Y. Fedorak, A. Escarpa, R. Vazquez-Duhalt and J. Wang, *Chem. – Eur. J.*, 2014, **20,** 2866-2871.
2 J. G. S. Moo and M. Pumera, *Chem. – Eur. J.*, 2015, **21,** 58-72.
3 A. Sen, M. Ibele, Y. Hong and D. Velegol, *Faraday Discuss.*, 2009, **143,** 15-27.
4 J. Wang, *Lab Chip*, 2012, **12,** 1944-1950.
5 D. Patra, S. Sengupta, W. Duan, H. Zhang, R. Pavlick and A. Sen, *Nanoscale*, 2013, **5,** 1273-1283.
6 J. Wang and W. Gao, *ACS Nano*, 2012, **6,** 5745-5751.
7 M. Pumera, *Nanoscale*, 2010, **2,** 1643-1649.
8 W. Wang, W. Duan, S. Ahmed, T. E. Mallouk and A. Sen, *Nano Today*, 2013, **8,** 531-554.
9 Y. Mei, A. A. Solovev, S. Sanchez and O. G. Schmidt, *Chem. Soc. Rev.*, 2011, **40,** 2109-2119.
10 L. Soler and S. Sanchez, *Nanoscale*, 2014, **6,** 7175-7182.
11 W. Gao and J. Wang, *ACS Nano*, 2014, **8,** 3170-3180.
12 W. Gao, S. Sattayasamitsathit, J. Orozco and J. Wang, *J. Am. Chem. Soc.*, 2011, **133,** 11862-11864.
13 S. Sanchez, A. N. Ananth, V. M. Fomin, M. Viehrig and O. G. Schmidt, *J. Am. Chem. Soc.*, 2011, **133,** 14860-14863.
14 H. Wang, G. Zhao and M. Pumera, *J. Am. Chem. Soc.*, 2014, **136,** 2719-2722.
15 H. Wang, J. G. S. Moo and M. Pumera, *Nanoscale*, 2014, **6,** 11359-11363.
16 K. M. Manesh, M. Cardona, R. Yuan, M. Clark, D. Kagan, S. Balasubramanian and J. Wang, *ACS Nano*, 2010, **4,** 1799-1804.
17 A. A. Solovev, Y. Mei, E. Bermúdez Ureña, G. Huang and O. G. Schmidt, *Small*, 2009, **5,** 1688-1692.
18 V. M. Fomin, M. Hippler, V. Magdanz, L. Soler, S. Sanchez and O. G. Schmidt, *IEEE Trans. Robot.*, 2014, **30,** 40-48.
19 J. G. S. Moo, H. Wang, G. Zhao and M. Pumera, *Chem. – Eur. J.*, 2014, **20,** 4292-4296.
20 B. Jurado-Sánchez, S. Sattayasamitsathit, W. Gao, L. Santos, Y. Fedorak, V. V. Singh, J. Orozco, M. Galarnyk and J. Wang, *Small*, 2015, **11,** 499-506.
21 J. Li, V. V. Singh, S. Sattayasamitsathit, J. Orozco, K. Kaufmann, R. Dong, W. Gao, B. Jurado-Sanchez, Y. Fedorak and J. Wang, *ACS Nano*, 2014, **8,** 11118-11125.
22 L. Soler, V. Magdanz, V. M. Fomin, S. Sanchez and O. G. Schmidt, *ACS Nano*, 2013, **7,** 9611-9620.
23 J. Orozco, G. Cheng, D. Vilela, S. Sattayasamitsathit, R. Vazquez-Duhalt, G. Valdés-Ramírez, O. S. Pak, A. Escarpa, C. Kan and J. Wang, *Angew. Chem., Int. Ed.*, 2013, **52,** 13276-13279.
24 J. Orozco, B. Jurado-Sánchez, G. Wagner, W. Gao, R. Vazquez-Duhalt, S. Sattayasamitsathit, M. Galarnyk, A. Cortés, D. Saintillan and J. Wang, *Langmuir*, 2014, **30,** 5082-5087.
25 G. Zhao and M. Pumera, *Lab Chip*, 2014, **14,** 2818-2823.
26 G. Zhao and M. Pumera, *RSC Adv.*, 2013, **3,** 3963-3966.